Highly oriented crystals at the buried interface in polythiophene thin-film transistors

R. JOSEPH KLINE[1], MICHAEL D. MCGEHEE[1]* AND MICHAEL F. TONEY[2]

[1]Department of Materials Science and Engineering, Stanford University, Stanford, California 94305, USA

[2]Stanford Synchrotron Radiation Laboratory, Menlo Park, California 94025, USA

*e-mail: mmcgehee@stanford.edu

Published online: 19 February 2006; doi:10.1038/nmat1590

Thin films of polymer semiconductors are being intensively investigated for large-area electronics applications such as light-emitting diodes, photovoltaic cells and thin-film transistors. Understanding the relationship between film morphology and charge transport is key to improving the performance of thin-film transistors. Here we use X-ray diffraction rocking curves to provide direct evidence for highly oriented crystals at the critical buried interface between the polymer and the dielectric where the current flows in thin-film transistors. Treating the substrate surface with self-assembled monolayers significantly varies the concentration of these crystals. We show that the polymer morphology at the buried interface can be different from that in the bulk of the thin films, and provide insight into the processes that limit charge transport in polythiophene films. These results are used to build a more complete model of the relationship between chain packing in polymer thin-films and charge transport.

Conjugated polymers are being developed as an alternative to amorphous silicon for the active layer of thin-film transistors (TFTs) for large-area and low-cost applications, including flat-panel displays and radiofrequency identification tags[1–4]. Although the manufacturing costs for conjugated polymers will probably be lower than for amorphous silicon, the charge-carrier mobility is not as high. Understanding the factors that limit the charge-carrier mobility is critical to improving performance and making conjugated polymer TFTs useful. Control of polymer crystallinity, crystal orientation and morphology has been shown to be important for obtaining high charge-carrier mobility[5–8]. The current in bottom-gated TFTs only travels in the region of the polymer film within approximately 5 nm (1–2 monolayers) of the gate dielectric[9]. Therefore, the polymer morphology at this buried interface controls charge transport in a TFT whereas that in the rest of the film has little effect. As the structure of the first few monolayers could be different from the rest of the 20–50 nm film, it is crucially important to separate the bulk structure from the interfacial structure.

Most studies of conjugated polymer TFTs have used silicon oxide as the gate dielectric and not the low-cost polymer dielectrics that will probably be required for commercial applications. Treating the silicon oxide substrate with hexamethyldisilizane (HMDS) has been shown to enhance the charge-carrier mobility of poly(3-hexylthiophene) (P3HT) by a factor of two[10]. Treating the silicon oxide surface with self-assembled monolayers (SAMs) has been shown to enhance the charge-carrier mobility of both poly(9,9′-dioctylfluorene-co-2,2′-bithiophene)[11] and poly[5,58-bis(3-alkyl-2-thienyl)-2,28-bithiophene)] (PQT)[12]. Other groups have also observed that the mobility of P3HT and PQT can be improved by surface treatment of the dielectric[13–15]. A method for using poly(dimethylsiloxane) has been developed to delaminate and transfer a PQT film to a new set of electrodes[16]. Transferring a PQT film cast on a SAM to a bare oxide substrate does not reduce the charge-carrier mobility, but annealing the transferred film on the bare oxide surface reduces the mobility to the value expected for bare oxide. These observations show that the effect of the dielectric surface on charge transport is due to surface-induced morphology

and not charge trapping. Reduced charge-carrier mobilities have been reported for P3HT films deposited on polymer dielectrics, and it has been suggested that substrate-driven morphological effects limit the charge transport[17]. Most other reports of polymer TFTs with polymer dielectrics have also shown reduced mobilities compared with those using inorganic substrates[13,18–20]. Although it is believed that the substrate influences the charge transport through the morphology, the structure of the buried layer has not been reported so far as all morphology measurements used until now characterize the entire film. A technique for directly measuring the first few monolayers of the polymer film is thus highly desirable for determining the influence of the substrate and improving the performance of polymer TFTs.

In this article, we present experimental evidence from X-ray diffraction (XRD) showing that the buried layer is different from the bulk in P3HT films cast on SAM-treated silicon oxide substrates. The data show that P3HT thin films have a surprisingly large population of highly oriented crystals. The degree of orientation of these crystals is similar to that observed for pentacene films[21]. Results showing that a preferred crystal orientation is critical for obtaining a high mobility in P3HT did not establish the degree of orientation present in these films[5]. In addition, it is likely that the enhanced mobilities obtained for P3HT cast on SAM-treated silicon oxide substrates are a direct result of these highly oriented crystals. These highly oriented crystals are not unique to P3HT, we have also observed them in both PQT and poly[5,5′-bis(4-decyl-2-thienyl)-2,2′thieno(2,3-b)thiophene] (M. Chabinyc, I. McCulloch, R.J.K., M.F.T., M.D.M., manuscript in preparation). Our results suggest that to transfer these high mobilities to films cast on polymer dielectrics, the polymer–polymer interface will need to be engineered to nucleate these oriented crystals. We have studied the field-effect mobilities obtained for films of P3HT spin-cast onto substrates treated with either HMDS or octadecyltrichlorosilane (OTS) to determine the effect of surface treatment on molecular packing and charge transport. The study was also done with various molecular weights, because we have shown that the molecular weight of the polymer has a tremendous effect on both the polymer morphology and charge-carrier mobility[7,22]. Figure 1 shows that the importance of the surface treatment for charge transport is strongly related to the molecular weight. Films with low ($M_{n,GPC} < 4$ kD) and medium ($M_{n,GPC} \sim 10$ kD) number-average molecular weights (as determined by gel-permeation chromatography, GPC) have a very large increase of mobility going from HMDS-treated to OTS-treated substrates, whereas films with high molecular weight ($M_{n,GPC} > 30$ kD) are not affected. This result is expected as the smaller molecules present in films with low and medium molecular weights should move much more easily, and can rearrange into a structure that optimizes the interaction between the polymer and the substrate surface[23]; this allows beneficial ordering on substrate surfaces and increases the mobility. The large molecules in the films with high molecular weight are expected to be kinetically limited from rearranging into a favourable interfacial packing arrangement.

As the charge transport in TFTs occurs in the plane of the substrate, grazing incidence X-ray scattering (GIXS) was used to characterize the in-plane π-stacking[5,7,24,25]. Films with a preferred orientation containing both the chain axis and the π-stacking direction in the plane of the film have been reported to have the highest mobilities because the charge can travel in two dimensions[5,6]. Figure 2 shows GIXS data comparing films cast on substrates treated with HMDS and OTS. The GIXS results show a change in the packing for the films with low molecular weight when going from an HMDS-treated to an OTS-treated substrate. The amount of in-plane π-stacking (010) increases whereas the in-plane

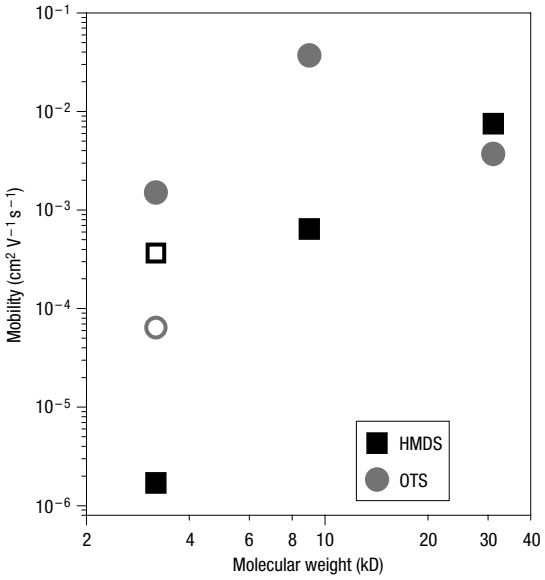

Figure 1 Effect of surface treatment on the charge transport of polymer films with various molecular weights. Filled symbols are for unannealed films. Open symbols are for the films with low molecular weight after annealing at 150 °C for 30 min. See Supplementary Information, Fig. S2 for TFT data.

side-chain packing (100) decreases when going to the OTS-treated substrate. This observed change in preferred orientation in the film and the 1,000-fold increase in mobility of low-molecular weight films on OTS-treated substrates were consistent with a previous model[5]. On the other hand, the GIXS results for the films with medium and high molecular weights show very little change for the different substrate treatments. This is not surprising for the films with high molecular weight, as the mobility was independent of surface treatment. This is surprising for the films with medium molecular weight, as a 100-fold increase in mobility was observed when going from an HMDS-treated substrate to an OTS-treated substrate. This finding shows that structural factors not revealed by GIXS are important to the charge-carrier mobility.

The conventional wisdom for conjugated polymer morphology is that the distribution of crystal orientations is large. As GIXS measures crystals with lattice planes perpendicular to the substrate (within about 0.7°), only a small portion of reciprocal space is sampled and it is likely that crystals not measured by GIXS are important for charge transport. Specular (out-of-plane) XRD can measure crystals with lattice planes normal to the substrate (within about 0.03°, depending on resolution). Rocking curves provide a means for measuring the distribution of crystal orientations in a film throughout reciprocal space. In a rocking-curve experiment, the sample is rotated in the X-ray beam while keeping the scattering angle (2θ) constant. Low-resolution rocking curves have been used to show a film processing-dependent distribution width that varied from 14 to 40° for P3HT[26].

Figure 3 shows the specular diffraction obtained for the (100) peak of films with various molecular weights on OTS-treated substrates. The peak intensity, width and position vary with molecular weight, with the films with low molecular weight having the highest integrated intensity, narrowest peaks and smallest d (lattice plane) spacing. The trend of reduced d spacing with films with low molecular weight has been reported previously[7,27], and is due to either a change in molecular tilt angle or amount of side-chain interdigitation. The reduced peak width indicates that

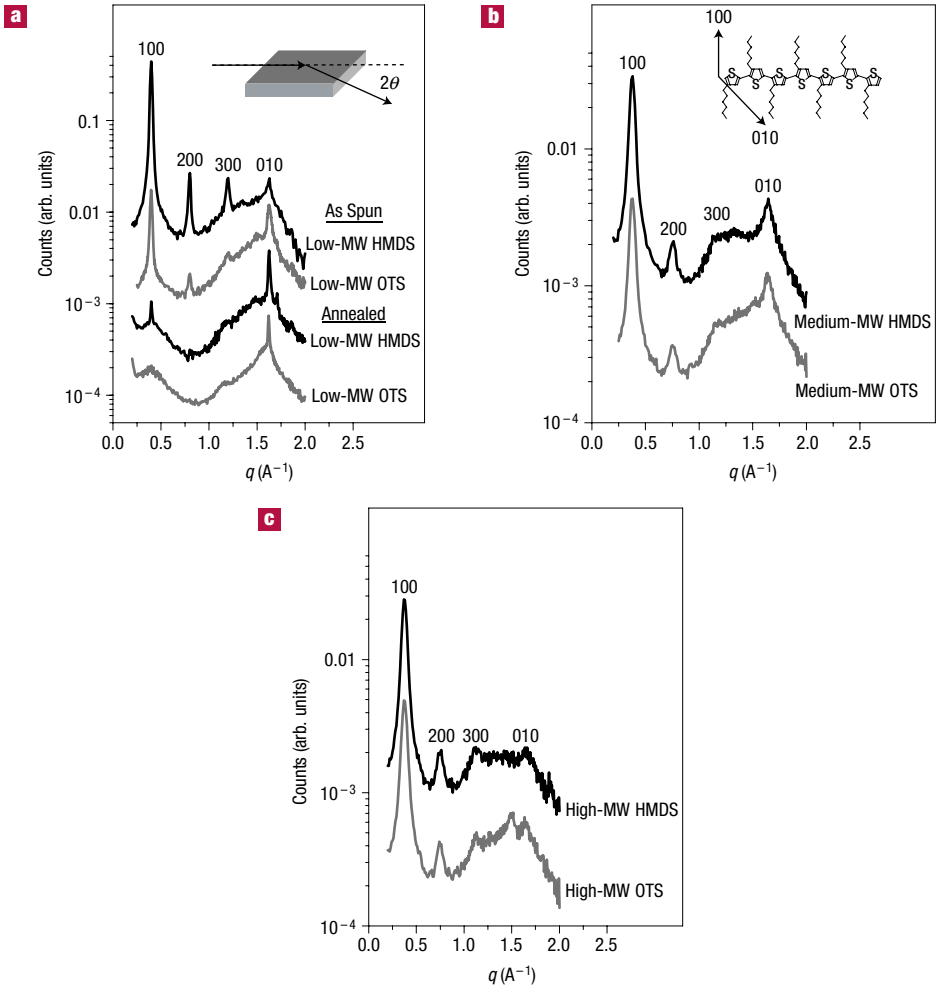

Figure 2 Effect of substrate and annealing on in-plane packing. In-plane diffraction on films of **a**, low molecular weight on HMDS-treated and OTS-treated substrate before and after annealing, **b**, medium molecular weight on HMDS and OTS and **c**, high molecular weight on HMDS and OTS. Data are plotted versus the scattering vector q. Insets in **a** and **b** show GIXS geometry and the molecular and crystal axes of P3HT, respectively.

the domain size perpendicular to the films is larger for films with low molecular weight than for those with medium and high molecular weights. Figure 4 shows the results of rocking-curve experiments measuring the orientation of the (100) packing relative to the substrate normal. The rocking curves consist of a sharp peak on a slowly varying background, with the sharp peak contributing to over 95% of the Bragg peak intensity of the specular measurement (Fig. 3). Figure 4a compares rocking curves of films with various molecular weights on OTS-treated substrates and shows that both the intensity of the peak and the background increase with decreasing molecular weight.

The sharp peaks in the rocking curves are caused by highly oriented crystals with a distribution width of less than 0.03°, corresponding to the resolution of our instrument. The only possible location to nucleate such highly oriented crystals is either the substrate or the air interface. Surface-induced ordering has been observed in liquid crystals and block copolymers at both the substrate and air interfaces, but the degree of orientation is less than we observe[28–31]. As the surface of the oxidized silicon substrate is smooth, with an atomic force microscope (AFM) measured r.m.s. roughness of about 1 Å, any possible orientation variations due to substrate roughness are negligible. The P3HT film surface,

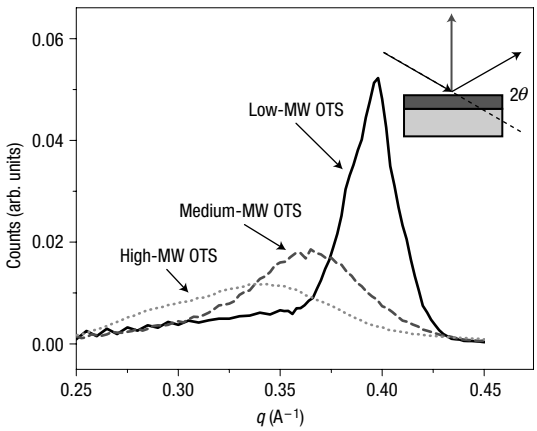

Figure 3 Specular diffraction of the ⟨100⟩ peak. Out-of-plane diffraction peaks analysed with rocking curves shown in Fig. 4 for the films with low, medium and high molecular weights on OTS-treated substrates. The inset shows the specular diffraction geometry.

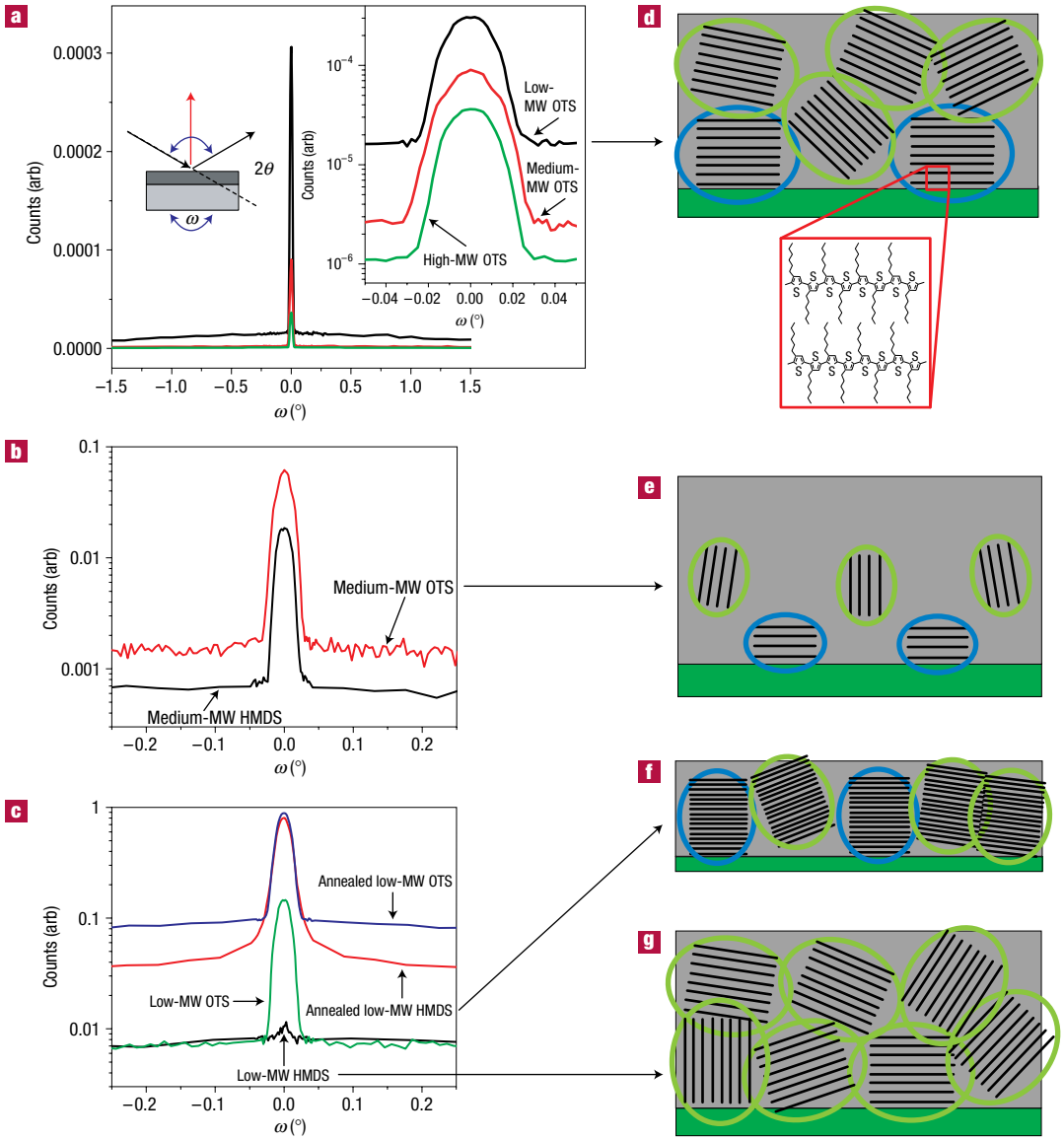

Figure 4 Rocking-curve measurements on the (100) peaks and resulting crystal orientations. a, Rocking curves for the films low, medium and high molecular weights on OTS-treated substrates. Left inset: the rocking curve geometry showing the angle relative to the sample normal ω. Right inset: a magnification of the $\omega = 0$ region plotted on a logarithmic scale. Logarithmic-scale rocking curves on films with **b**, medium molecular weight on both HMDS and OTS and **c**, low molecular weight before and after annealing for both HMDS and OTS. Schematics showing the highly oriented and misoriented crystals in films with **d**, low molecular weight on OTS, **e**, medium and high molecular weights on OTS, **g**, low molecular weight on HMDS before annealing and **f**, after annealing (drawn on a smaller scale to accommodate the larger crystals). Lines correspond to the (100) plane. Blue circles denote crystals measured by specular diffraction and green circles denote those that are not.

on the other hand, has an r.m.s. roughness measured by AFM of about 6 Å. Furthermore, AFM images show inclined crystals with surface slope variations of greater than 0.3°. As no crystal steps are observed with AFM, these slopes are due to changes in crystal orientation. These orientation variations of the crystals at the air–film interface are at least an order of magnitude greater than the width of the rocking-curves peaks. Thus, these observations suggest that the highly oriented crystals cannot be nucleated from the air–film interface. Further evidence that the crystals nucleate from the substrate is that the films cast on OTS-treated substrates have more oriented crystals than those cast on HMDS-treated substrates. The only difference between rocking curves of films with low molecular weight cast on HMDS and OTS substrates is that films cast on OTS have the peak associated with the highly oriented crystals (Fig. 4d,f). It is unlikely that the surface treatment of the substrate could affect nucleation at the air–film interface, so the only reasonable place for these highly oriented crystals to nucleate is the substrate.

The resolution-limited peak in the rocking scans shows that the lateral coherence length of the (100) planes is greater than about 10 μm (ref. 32). This coherence length is orders of magnitude larger than the 20–40 nm in-plane (010) domain size calculated from GIXS measurements. This discrepancy is explained by the fact that the coherence of out-of-plane (100) crystal planes does

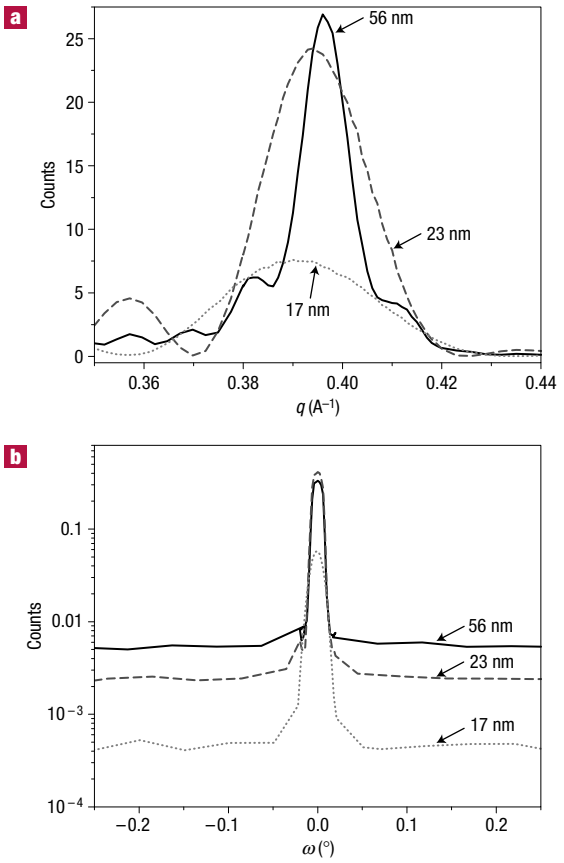

Figure 5 Specular diffraction and rocking curve of the ⟨100⟩ peak for various film thicknesses with low molecular weight. a, Out-of-plane diffraction for films with low molecular weight cast on OTS-treated substrates for various film thicknesses. **b**, Rocking curves on the same films showing that the misoriented crystals scale with film thickness.

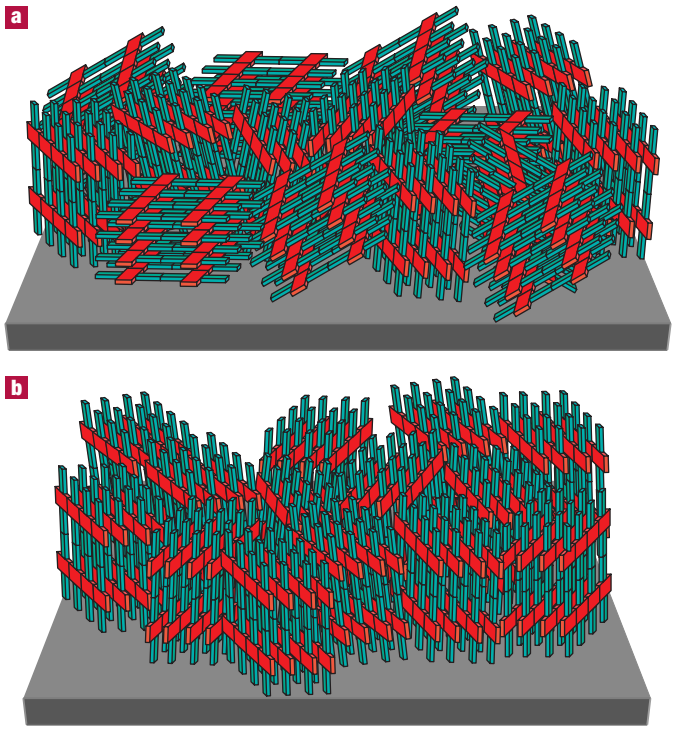

Figure 6 Schematic of possible packing arrangements of crystals at the buried interface of films with low molecular weight. a, Poor orientation. Variations of orientations at the interface of HMDS-treated substrates and the large number of grain boundaries with a (100) face. **b**, Good orientation. Preferentially oriented crystals at the interface of OTS-treated substrates with lots of grain boundaries with (010) and (001) faces. Conducting π-stacking planes are marked red and insulating hexyl chains are marked green. Crystals are reduced in size for clarity.

not require coherence in the in-plane (010) crystal planes. As the 1 Å roughness of the substrate is substantially less than the 15.5 Å d spacing, the (100) planes of neighbouring highly oriented grains are aligned with each other independent of their in-plane orientation. Some metallic thin-films grown from sapphire substrates have been shown to have lateral coherence lengths much larger than the crystal size[33,34].

As well as the sharp peaks, the rocking curves also have a non-zero background from a population of crystals with a much larger angular distribution than the highly oriented crystals. These marginally oriented crystals are nucleated either in the bulk film, at the air–film interface or in the solution before deposition. Some of these crystals are tilted 90° from the substrate normal giving rise to the (100) peaks in the GIXS data in Fig. 2. One way to show that the sharp peaks in the rocking curves come from oriented crystals at the bottom of the film and the broad background comes from the rest of the film is to analyse films of varying thickness. Figure 5 shows the specular diffraction and rocking curves from samples of low molecular weight of three different thicknesses. The (100) peak width increases with decreasing film thickness because the thinner films limit the domain size of the crystals. Rocking curves show that the background associated with marginally oriented crystals scales with film thickness. This trend in relative intensities of the background and peak with film thickness confirms that the poorly oriented crystals are primarily in the bulk film, whereas the well-oriented crystals are at the critical buried interface (Fig. 4d).

The fact that the film with low molecular weight cast on HMDS has few highly oriented crystals probably explains why the mobility is so much lower than the other films. This can be rationalized as follows. The anisotropy of P3HT crystals limits charge transport to two crystal directions (⟨010⟩ and ⟨001⟩) with the insulating hexyl chains preventing charge transport in the ⟨100⟩ direction. A large distribution of crystal orientations increases the likelihood of having poor electronic overlap along these high-mobility directions between neighbouring grains. Figure 6a and b compare the interfacial crystals present in films with low molecular weight cast both on HMDS and on OTS and shows that a large number of the crystals in films cast on HMDS-treated substrates will have insulating grain boundaries in the plane of charge transport. The highly oriented crystals of the films with low molecular weight cast on OTS, on the other hand, will have few insulating grain boundaries in the plane of charge transport.

Annealing has an interesting effect on the films with low molecular weight. After annealing, highly oriented crystals appear in the films with low molecular weight cast on HMDS, corresponding to an increase in the charge-carrier mobility. The rocking curve in Fig. 4c shows that both the peak associated with the highly oriented crystals and the broad scattering background associated with the marginally oriented crystals increase with annealing for both substrates for films with low molecular weight. The increase in the broad scattering in the measured angular

range indicates that more crystals have an orientation close to the substrate normal. The combination of these rocking-curve results along with the decrease of in-plane alkyl stacking and the increase of in-plane π-stacking peaks in the GIXS measurements (Fig. 2c,d) reveal a net change in the crystal orientations. The (100) peak widths of the out-of-plane XRD of films with low molecular weight decrease with annealing with both substrate treatments, indicating an increase in the size of these crystals (Fig. 4f,g). Charge-transport measurements (Fig. 1) show that mobility increases with annealing for the films with low molecular weight on HMDS, whereas it decreases on OTS. The decrease in mobility for OTS disagrees with the trend of mobility going up with an increase in the amount of highly oriented crystals. GIXS shows the film to primarily contain in-plane π-stacking with very little in-plane side-chain stacking. In all other cases, charge transport increased when the in-plane π-stacking increased for a constant molecular weight. Optical micrographs and AFM images of the film show that the film dewets during annealing and is no longer continuous (see Supplementary Information, Fig. S1). Thus, the reduction in mobility was a result of film discontinuity and not the chain packing.

Rocking curves show a clear difference between the two films with medium molecular weight that looked nearly identical in the GIXS measurements despite having substantially different charge-carrier mobilities (Fig. 4b). The film with medium molecular weight on OTS has more highly oriented crystals than that on HMDS. This increase in highly oriented crystals increases the mobility in the film by reducing the number of highly misoriented grain boundaries that have poor electronic overlap (see Fig. 6), and explains the 100-fold increase of mobility between the film with medium molecular weight on OTS and that on HMDS. The GIXS curves of the two films are similar because the scattering comes from the entire polymer film and the highly oriented crystals at the critical buried interface are only a small fraction of the film. The rocking-curve results indicate that the increased charge-carrier mobility often associated with increased in-plane π-stacking is actually due to the improved grain boundaries of the highly oriented crystals, and only indirectly related to the in-plane π-stacking. The highly oriented nature of the crystals at the buried interface makes rocking curves a sensitive tool for measuring them separately from the rest of the film. In cases where GIXS measurements cannot fully explain variations in charge transport, rocking curves can provide further information about the morphology. Measurements such as these will be critical to the development of polymer dielectrics for high-mobility conjugated polymers.

METHODS

SUBSTRATE PREPARATION AND DEVICE TESTING

Substrates for X-ray measurements were cleaned silicon ⟨100⟩ wafers (Silicon Quest) with a thin oxide layer (~2 nm) grown by exposure to ultraviolet ozone for 30 min. TFTs were bottom-contact, bottom-gated structures using a highly doped ⟨100⟩ wafer as the gate, 300-nm of thermally grown oxide as the gate dielectric, and a photolithographically patterned gold/titanium layer as the source/drain electrodes. Hexamethyldisilizane (Aldrich) was deposited by spin-coating from a 100% solution at 5,000 r.p.m. and had a water contact angle of ~70°. Octadecyltrichlorosilane (Aldrich) was deposited by immersing the substrate in a 1 mM hexadecane solution (Aldrich) for 10 min and had a water contact angle of >110°. Substrates were then rinsed in hexane and isopropanol followed by blowing with dry nitrogen. Polymer films were spin-coated in a nitrogen purged glove box at 2,500 r.p.m. from chloroform. Polymer films were 30–60 nm thick. Polymers used were synthesized by the modified McCullough route as described previously[35]. The polymers were classified as low ($M_{n,GPC}$ < 4 kD), medium ($M_{n,GPC}$ ~ 10 kD) and high-molecular weight ($M_{n,GPC}$ > 30 kD). TFT measurements were performed under vacuum in a cryostat (Janus STS-450). Reported mobilities were calculated in the saturation regime by fitting the data to the saturation regime:

$$I_{ds} = \frac{W}{2L} C_i \mu \left(V_g - V_t\right)^2, \quad (1)$$

where I_{ds} is the drain current in saturation, W is the channel width, L is the channel length, C_i is the capacitance of the insulator, μ is the charge carrier mobility, V_g is the gate voltage and V_t is the threshold voltage.

MORPHOLOGY CHARACTERIZATION

X-ray measurements were performed at the Stanford Synchrotron Radiation Laboratory on beam line 7-2 at an energy of 8 keV. Samples were tested in ambient flowing helium to prevent the beam from damaging the sample. Rocking curves were measured in the specular setup looking at the ⟨100⟩ peak. The background reflectivity was measured adjacent to the Bragg peak and subtracted from the rocking-curve measurement. In most cases, the reflectivity was substantially less than the Bragg intensity (<1%). The rocking curves were corrected for changes in sample illumination area by multiplying the data by θ. GIXS was carried out with an incident angle of 0.2° and a scattered beam resolution of 1 mrad. The incident angle corresponds to a penetration depth of the entire polymer film and 10 nm in the silicon substrate. GIXS data were corrected for changes in sample illumination[36].

Received 25 July 2005; accepted 6 January 2006; published 19 February 2006.

References

1. Horowitz, G. Organic thin film transistors: From theory to real devices. *J. Mater. Res.* **19,** 1946–1962 (2004).
2. Chabinyc, M. L. & Salleo, A. Materials requirements and fabrication of active matrix arrays of organic thin-film transistors for displays. *Chem. Mater.* **16,** 4509–4521 (2004).
3. Katz, H. & Bao, Z. The physical chemistry of organic field-effect transistors. *J. Phys. Chem. B* **104,** 671–678 (2000).
4. Dimitrakopoulos, C. & Malenfant, P. Organic thin film transistors for large area electronics. *Adv. Mater.* **14,** 99–117 (2002).
5. Sirringhaus, H. *et al.* Two-dimensional charge transport in self-organized, high-mobility conjugated polymers. *Nature* **401,** 685–688 (1999).
6. Chang, J. F. *et al.* Enhanced mobility of poly(3-hexylthiophene) transistors by spin-coating from high-boiling-point solvents. *Chem. Mater.* **16,** 4772–4776 (2004).
7. Kline, R. J. *et al.* Dependence of regioregular poly(3-hexylthiophene) film morphology and field-effect mobility on molecular weight. *Macromolecules* **38,** 3312–3319 (2005).
8. Sirringhaus, H. *et al.* Mobility enhancement in conjugated polymer field-effect transistors through chain alignment in a liquid-crystalline phase. *Appl. Phys. Lett.* **77,** 406–408 (2000).
9. Tanase, C., Blom, P. W. M., De Leeuw, D. M. & Meijer, E. J. Charge carrier density dependence of the hole mobility in poly(*p*-phenylene vinylene). *Phys. Status Solidi A* **201,** 1236–1245 (2004).
10. Sirringhaus, H., Tessler, N. & Friend, R. H. Integrated optoelectronic devices based on conjugated polymers. *Science* **280,** 1741–1744 (1998).
11. Salleo, A., Chabinyc, M., Yang, M. & Street, R. Polymer thin-film transistors with chemically modified dielectric interfaces. *Appl. Phys. Lett.* **81,** 4383–4385 (2002).
12. Salleo, A. *et al.* Intrinsic hole mobility and trapping in a regioregular poly(thiophene). *Phys. Rev. B* **70,** 115311 (2004).
13. Veres, J., Ogier, S., Lloyd, G. & De Leeuw, D. Gate insulators in organic field-effect transistors. *Chem. Mater.* **16,** 4543–4555 (2004).
14. Wu, Y. *et al.* Controlled orientation of liquid-crystalline polythiophene semiconductors for high-performance organic thin-film transistors. *Appl. Phys. Lett.* **86,** 1–3 (2005).
15. Kim, D. H. *et al.* Enhancement of field-effect mobility due to surface-mediated molecular ordering in regioregular polythiophene thin film transistors. *Adv. Mater.* **15,** 77–82 (2005).
16. Chabinyc, M. L. *et al.* Lamination method for the study of interfaces in polymeric thin film transistors. *J. Am. Chem. Soc.* **126,** 13928–13929 (2004).
17. Chua, L. L. *et al.* General observation of n-type field-effect behaviour in organic semiconductors. *Nature* **434,** 194–199 (2005).
18. Rost, H., Ficker, J., Alonso, J. S., Leenders, L. & Mcculloch, L. Air-stable all-polymer field-effect transistors with organic electrodes. *Synth. Met.* **145,** 83–85 (2004).
19. Park, S. K., Kim, Y. H., Han, J. I., Moon, D. G. & Kim, W. K. High-performance polymer TFTs printed on a plastic substrate. *IEEE Trans. Electron Dev.* **49,** 2008–2015 (2002).
20. Park, J., Park, S. Y., Shim, S. O., Kang, H. & Lee, H. H. A polymer gate dielectric for high-mobility polymer thin-film transistors and solvent effects. *Appl. Phys. Lett.* **85,** 3283–3285 (2004).
21. Nickel, B. *et al.* Dislocation arrangements in pentacene thin films. *Phys. Rev. B* **70,** 125401 (2004).
22. Kline, R. J., Mcgehee, M. D., Kadnikova, E. N., Liu, J. & Frechet, J. M. J. Controlling the field-effect mobility of regioregular polythiophene by changing the molecular weight. *Adv. Mater.* **15,** 1519–1522 (2003).
23. Knaapila, M. *et al.* The influence of the molecular weight on the thermotropic alignment and self-organized structure formation of branched side chain hairy-rod polyfluorene in thin films. *Macromolecules* **38,** 2744–2753 (2005).
24. Aasmundtveit, K. E. *et al.* Structural anisotropy of poly(alkylthiophene) films. *Macromolecules* **33,** 3120–3127 (2000).
25. Winokur, M. J. & Chunwachirasiri, W. Nanoscale structure-property relationships in conjugated polymers: implications for present and future device applications. *J. Polym. Sci. B* **41,** 2630–2648 (2003).
26. Yang, H. *et al.* Effect of mesoscale crystalline structure on the field-effect mobility of regioregular poly(3-hexyl thiophene) in thin-film transistors. *Adv. Funct. Mater.* **15,** 671–676 (2005).
27. Zen, A. *et al.* Effect of molecular weight and annealing of poly(3-hexylthiophene)s on the performance of organic field-effect transistors. *Adv. Funct. Mater.* **14,** 757–764 (2004).
28. Lang, P. Surface induced ordering effects in soft condensed matter systems. *J. Phys. Condens. Matter* **16,** R699–R720 (2004).
29. Brown, G. & Chakrabarti, A. Surface-induced ordering in block copolymer melts. *J. Chem. Phys.* **101,** 3310–3317 (1994).

30. Gutman, L. & Chakraborty, A. K. Surface-induced ordering for confined random block copolymers. *J. Chem. Phys.* **101,** 10074–10091 (1994).
31. Factor, B. J., Russell, T. P. & Toney, M. F. Surface-induced ordering of an aromatic polyimide. *Phys. Rev. Lett.* **66,** 1181–1184 (1991).
32. Munkholm, A., Brennan, S. & Carr, E. C. A comparison of surface roughness as measured by atomic force microscopy and X-ray scattering. *J. Appl. Phys.* **82,** 2944–2953 (1997).
33. Nefedov, A., Abromeit, A., Morawe, C. & Stierle, A. High-resolution X-ray scattering study of platinum thin films on sapphire. *J. Phys. Condens. Matter* **10,** 717–730 (1998).
34. Wolfing, B., Theis-Brohl, K., Sutter, C. & Zabel, H. AFM and X-ray studies on the growth and quality of Nb(110) on alpha-Al{sub 2}O{sub 3}(1120). *J. Phys. Condens. Matter* **11,** 2669–2678 (1999).
35. Liu, J. S., Sheina, E., Kowalewski, T. & Mccullough, R. D. Tuning the electrical conductivity and self-assembly of regioregular polythiophene by block copolymerization: Nanowire morphologies in new di- and triblock copolymers. *Angew. Chem. Int. Edn* **41,** 329–332 (2002).
36. Toney, M. F. & Wiesler, D. G. Instrumental effects on measurements of surface X-ray diffraction rods: resolution function and active sample area. *Acta Crystallogr. A* **49,** 624–642 (1993).

Acknowledgements

We acknowledge M. Chabinyc for assistance in OTS deposition, J. Fréchet for providing the polymers and B. Clemens for discussion on the rocking curves. Financial support was provided by National Science Foundation MRSEC Program (award number DMR-0213618), the Department of Energy and Xerox Corporation. Portions of this research were carried out at the Stanford Synchrotron Radiation Laboratory, a national user facility operated by Stanford University on behalf of the US Department of Energy, Office of Basic Energy Sciences.
Correspondence and requests for materials should be addressed to M.D.M.
Supplementary Information accompanies this paper on www.nature.com/naturematerials.

Competing financial interests

The authors declare that they have no competing financial interests.